

Electron Channels in Biomolecular Nanowires

Arrigo Calzolari,^{*,†} Rosa Di Felice,[†] Elisa Molinari,^{†,§} and Anna Garbesi^{†,‡}

INFM Center for nanoStructures and bioSystems at Surfaces (*S*³), and Dipartimento di Fisica, Università di Modena e Reggio Emilia, via Campi 213a, 41100 Modena, Italy, and CNR ISOF, Area della Ricerca, via Gobetti 101, 40129 Bologna, Italy

Received: September 9, 2003; In Final Form: December 15, 2003

We report a first-principle study of the electronic and conduction properties of a quadruple-helix guanine wire (G4 wire), a DNA derivative, with inner potassium ions. The analysis of the electronic structure highlights the presence of energy manifolds that are equivalent to the bands of (semi)conducting materials and reveals the formation of extended electron channels available for charge transport along the wire. The specific metal–nucleobase interactions affect the electronic properties at the Fermi level, leading the wire to behave as an intrinsically p-doped system.

1. Introduction

Fueled by the ever increasing drive for miniaturization and improved performance in electronic devices and by potential applications in the nanotechnologies, the research effort to investigate the properties of novel nanowire materials is undergoing an impressive growth. It is foreseen that the conventional solid-state technology could be replaced by new generations of devices based on molecular components, which take advantage of the quantum mechanical effects that rule the nanometer scale. Molecular electronics¹ is currently explored as a long-term alternative for increasing the device density in integrated circuits. However, to keep up with these expectations, the new trend must provide flexible, reproducible, and well structured architectures, easy to wire in a programmable way.

By virtue of their recognition and self-assembling properties, DNA molecules seem particularly suitable to fulfill these requirements. Both the intrinsic combinatorial principles of nucleic acids and their chemistry can be exploited to build precise, miniaturized, and locally modulated patterns, where the drawing of functional arrays is obtained through a series of programmed chemical reactions and not by the physical handling of the samples. The realization of DNA-based wired architectures via self-assembly is a viable route to scale down the size of devices to the molecular level.^{2–4} However, whereas it was demonstrated that the self-assembling capabilities of DNA make it suitable as a template to wire metallic materials,⁵ its ability as an intrinsic conductor is questioned by experimental results.⁶ Depending on base sequence, molecule length, environmental conditions, substrates, and electrode materials, the direct measurements of the dc conductivity of DNA-based structures in solid-state devices⁷ report insulating character,⁸ semiconductor-like transport characteristics,⁹ ohmic behavior,¹⁰ and proximity-induced superconductivity.¹¹ Indeed, even in the cases in which charge transport has been observed, the current is very low, with resistances of the order of 0.1–1 GΩ across the length of the DNA molecules (variable between 10 μm and 10 nm).

Thus, due to its apparent poor intrinsic conductivity, DNA might be reasonably considered as a bad insulator rather than a viable electrical molecular wire.

Besides the standard DNA, other nucleotide-based helical molecules, such as guanine quadruple helices (G4 wires) or “metal-manipulated” duplexes, may offer the desired mechanical, recognition, and self-assembly properties that make DNA so attractive. With respect to native DNA, these derivatives have metal cations in the inner core of the base stack. Whereas the interactions between *external* ions and the double helix have been largely studied both experimentally and theoretically, the effects of their inclusion *inside* the helix are largely unknown. The presence of *internal* metal ions may drastically affect the bonding pattern with and among the bases, introducing novel features in the structural and electronic properties of the system.¹² A promising pathway for the exploitation of DNA as a conductor in molecular devices is indicated by the evidence that metal ions incorporated in the helix core may modify the conductivity of DNA-based wires.^{13,14}

In this paper, we focus on nanowires known as G4 wires¹⁵ (or *quadruplexes*), consisting of stacked guanine (G) tetrads (G4): the structure of these systems is illustrated and described in Figure 1. These one-dimensional polymers are becoming appealing as prospective candidates for biomolecular electronics because, due to the low ionization potential of guanine (the lowest among nucleic-acid bases), they might be suitable to mediate charge transport by hole conduction along the helix and have even been suggested as nanomechanical extension–contraction machines.¹⁶ In the presence of appropriate metal cations (especially K⁺ and Na⁺), solutions of homoguanilyc strands in water,^{17,18} as well as lipophilic guanosine monomers in organic solvents,¹⁹ self-assemble in right-handed quadruple helices. The G4 motif has been identified in both cases; however, although the quadruplexes obtained from guanylate strands have an outer mantle of sugars and phosphates (as in DNA) that connects the adjacent G4 planes, those obtained from lipophilic guanosine derivatives have no interplanar connection: a continuous linker between consecutive tetramers is not necessary to form the wires. The guanine quadruplexes have recently attracted interest because of their possible role in biological systems;²⁰ their biological relevance has propelled a large number of investigations (e.g., X-ray²¹ and NMR²²) aimed at

* Corresponding author. E-mail: calzolari.arrigo@unimore.it. Phone: +39-059-2055627. Fax: +39-059-374794. URL: <http://www.s3.infm.it>.

† INFM Center for nanoStructures and bioSystems at Surfaces (*S*³).

§ Dipartimento di Fisica, Università di Modena e Reggio Emilia.

‡ CNR ISOF.

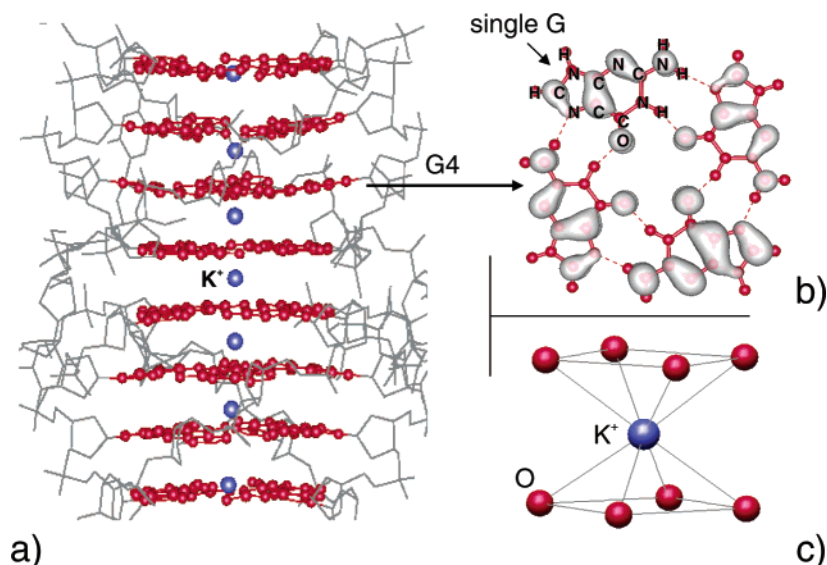


Figure 1. (a) Side view of a short quadruplex from which the simulated G4 wire was extracted. The image was derived from an experimental X-ray structure.²¹ The central core of the helix (red) is constituted of stacked supramolecular structures, the G quartets (G4), and the K⁺ ions (blue spheres) are hosted in the central cavity of the G quartet stack. The lateral gray sticks describe the external sugar-phosphate backbone, excluded in our simulations. By virtue of the overall C₄ symmetry of the helix, it is possible to extract a periodic unit of three G4 tetrads from this finite quadruplex, which constitutes the elementary building block of the simulated infinite wires. (b) Isolated G quartet that forms one plane of the stacked G4 wire. Each G4 consists of four coplanar H-bonded guanines, arranged in a square-like configuration. The image shows the relaxed geometry and an isosurface plot of the HOMO manifold. (c) Scheme of the bipyramidal K⁺-O coordination.

characterizing such unusual supramolecular structures. Quadruple helices have been obtained in the presence of different monovalent (K⁺, Na⁺, NH₄⁺)^{19a,23} and divalent (Ca²⁺, Ba²⁺, Sr²⁺, Pb²⁺)^{19b,24} cations. Despite the different chemical nature of the constituents, all these G4 wires are characterized by an inner core of stacked G4's intercalated by metal cations: one cation in *every* tetrad and one cation in *every other* tetrad, in the case of *mono*- and *divalent* ions, respectively. The self-assembly capability of the G4 helices allows for the formation of quite long (100–1000 nm) and stiff wires. AFM images²⁵ of four-stranded helices obtained from G-rich oligonucleotides on substrates revealed the G4 wires to be uniform and relatively rigid polymers, with few bends, kinks, or branches.

Despite the large amount of structural investigations, the conduction properties of these nanowires are basically unknown and a direct measurement of electrical properties of G4 wires is still missing. From the theoretical point of view, quantum chemistry and molecular dynamics studies focused on the energetics and on the geometry of isolated G quartets or finite clusters of stacked G4's,²⁶ whereas the electronic properties of these materials were so far investigated to a much lesser extent.²⁷

In the following, we present a first-principles investigation of the electronic and conduction properties of periodically repeated G4 wires. Recently,²⁷ we described the structure and the energetics, as well as some basic features of the electronic structure, of an infinite G4 wire with and without the presence of K⁺ ions in the inner cavity. In this paper, we focus entirely on the electronic properties of the same system and present a complete and thorough analysis of the guanine-guanine and metal-guanine interactions, discussing the effects on the conduction properties of the tubular system.

2. Computational Approach

We performed *ab initio* calculations of the electronic and conduction properties of infinite G4 wires in the presence of K⁺ ions, within the density functional theory (DFT) approach,²⁸ using the PW91²⁹ gradient-corrected exchange-correlation functional. DFT is lately gaining large credit in the scientific

community as a reliable and accurate method to describe large-scale biomolecular aggregates,³⁰ including guanine-based stacks.³¹

Our total-energy-and-force calculations³² allowed us to attain a simultaneous description of the optimized atomic configuration and of the corresponding electronic structure for the selected systems (see Figure 1): the finite planar guanine tetrad (G quartet) and the infinite helical G4 wire filled with K⁺ ions in the inner cavity (label 3G4/K⁺). The single-particle electron wave functions were expanded in a plane-wave basis set with a kinetic-energy cutoff of 25 Ry. Two special **k**-points in the irreducible wedge were employed for Brillouin zone (BZ) sums in the case of the G4 wire. The infinite helix was simulated by a repeated supercell containing three stacked G4 tetrads,²⁷ employing periodic boundary conditions in the three spatial directions. A thick vacuum layer (~16.0 Å) in the directions perpendicular to the helical axis prevented spurious interactions between adjacent replicas of the wire. For the isolated G quartet, the same vacuum thickness was employed also in the third direction perpendicular to the plane of the tetrad, and only the Γ point was used in the BZ sampling.

The electron-ion interaction was described by non-norm-conserving pseudopotentials³³ for all the species (C, N, O, H) except K, for which a norm-conserving pseudopotential³⁴ was used. For the latter species, both the valence 4s and the semicore 3p shells contributed to the system with valence electrons. This treatment represented a significant refinement toward a complete description of the electronic structure, with respect to the simplified results²⁷ obtained by fixing the 3p shell in the frozen core and by applying *Non Linear Core Corrections*³⁵ (NLCC) to account for partial core relaxation.

The starting atomic configuration was obtained from the results of the X-ray analysis²¹ of the d(TG₄T) quadruple helix. Motivated by the observation that G4 wires form with^{17,18} and without¹⁹ the covalent skeleton and by our specific interest in the base stack as a channel for charge mobility, we neglected the external backbone in our simulations and focused on the central core of the helix, constituted of guanines and metal cations (see Figure 1a). This choice is supported by theoretical

reports³⁶ for approximated DNA structural models, which assert that if any current flows in such systems, it does so through the base-stacking, without involving the external mantle in the transport phenomena. The same evidence was more recently confirmed by DFT calculations of the electronic properties of real DNA sequences (A-DNA^{8a} and Z-DNA³⁷): these simulations showed that the orbitals related to the sugar–phosphate backbone are a few electronvolts below the highest occupied molecular orbital (HOMO) and above the lowest unoccupied molecular orbital (LUMO) of the system. In principle, one should expect that the environment surrounding the base stack plays an important role in the overall conductivity properties of DNA molecules.^{37–39} Recent studies^{37,39b} pointed out that a random distribution of counterions in the unit cell modifies the electrical properties of DNA both reducing the *bulk* quantum conductance and introducing localized empty states in the energy gap. However, this result is coherent with a picture where the external ions *quantitatively* affect the global transport properties of the system but do not constitute an alternative pathway for the electron/hole transport through the helix.⁷ Therefore, we believe that the *bare* guanine core will be well representative of the essential electronic properties of the quadruplexes, allowing for the inspection of the charge-migration mechanisms and of the key features of metal–molecule interaction. An explicit account for the effects of the backbone and of the surrounding counterions^{37,39} would instead be demanded for a quantitative evaluation of the quantum conductance to be compared with measured transport characteristics, which is way beyond the purpose of the present work.

3. Results and Discussion

By means of the first-principle approach outlined above, we optimized both the isolated G quartet and the periodic G4 stack.

The analysis of the electronic structure of the planar G quartet shows interesting features that will help understanding the electrical properties of G4 wires. As also found for the other planar G aggregates (e.g., dimers, ribbons),³¹ the H-bonds among the guanines do not favor the formation of supramolecular orbitals extended on the whole G quartet and the existence of dispersive bands. On the other hand, the intermolecular interactions split each guanine energy level into a multiplet structure: each multiplet is composed of four (the number of G's in the tetrad) energy levels and has a total width of about 200 meV. The orbitals that contribute to a manifold have identical character and are localized on the individual G molecules. Figure 1b shows an isosurface plot of the convolution of four electron states (the HOMO's of the four guanines in the tetrad) which form the π -like HOMO manifold.

By exploiting the square symmetry of the planar tetrad and the 30° twist angle between consecutive tetrads, we simulated a quadruplex of infinite length with a periodically repeated unit supercell containing three stacked G quartets and three intercalated K⁺ ions in the unit cell.²⁷ Each potassium ion was symmetrically located between two consecutive tetrads, and bipyramidally coordinated with the eight (four above and four below) nearest-neighboring oxygen atoms (Figure 1c). The atomic positions were relaxed until the forces vanished, within an accuracy of 0.03 eV/Å. The structure, the energetics, and the metal-induced stability of the tube were described elsewhere.²⁷ We find now that the explicit inclusion of the semicore 3p electrons of K in the valence shell for the pseudopotential calculations does not alter the results obtained previously within the NLCC approximation²⁷ and does not change the understanding of the system from the structural point of view. The refined

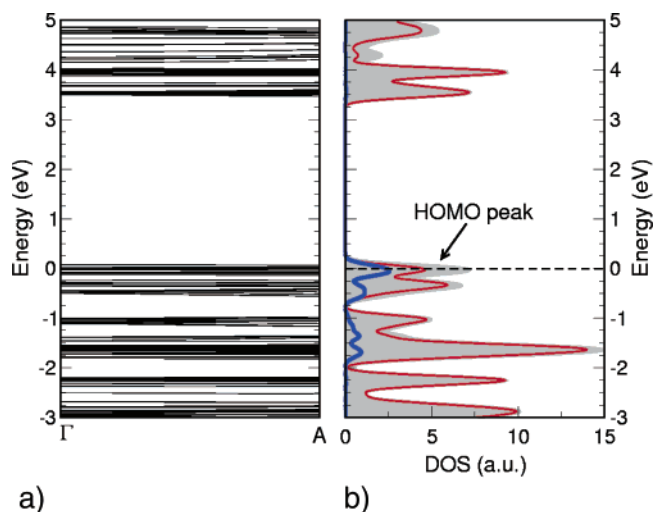


Figure 2. (a) Band structure along the Γ A direction parallel to the axis of the 3G4/K⁺ G4 wire, which coincides with the direction along which the planar tetrads stack. (b) Total and projected density of states (DOS) of the wire. The shaded gray area represents the total DOS. The thin red (thick blue) solid curve marks the projection of the DOS onto G (K). Note that the total DOS and the G-DOS coincide in a large part of the spectrum, where the thin red curve almost coincides with the border of the shaded area. The dashed horizontal curve indicates the Fermi level.

treatment of the semicore 3p electrons of K allows us to gain a deeper insight into the electronic structure.

The band structure of the G4 wire 3G4/K⁺ is shown in Figure 2a: the unoccupied states (above 3.5 eV) are separated from the occupied states (below 0 eV) by a large energy gap (affected by the typical DFT underestimation²⁸) and some of the states around zero energy are partially filled. We previously demonstrated³¹ that π – π coupling among guanines may give rise to delocalized Bloch-type orbitals, whose band dispersion along the stacking direction depends on the relative rotation angle between nucleobases in adjacent planes. Taking into account the detected rotation angle²¹ of 30° for the guanine quadruple helices, we now report that the electronic band structure of the 3G4/K⁺ column is represented by dispersionless energy bands, indicating that no complete supramolecular orbital delocalization is to be expected for such a degree of helicity. This behavior leads to the conclusion that in G4 wires the π – π superposition is not sufficient to induce a sizable coupling between the molecular states of guanines and/or the atomic orbitals of potassium, which would lead to *purely* dispersive bands similar to those of (semi)conducting materials. However, as for the isolated G quartet, the band structure of the 3G4/K⁺ column identifies the presence of manifolds that are equivalent to effective bands: each manifold contains a number (or multiplet) of levels that can be explained in terms of the number of nucleobase molecules and of potassium ions in the periodic supercell, as we discuss later. The orbitals in a multiplet have identical symmetries and some degree of hybridization between neighboring bases. The levels within a manifold are so close (dense) in energy ($\Delta E \leq 20$ meV) that an external weak interaction (e.g., the thermal fluctuations, an external electric field, etc.) may let the orbitals mix, giving an *effective* dispersive band. This interpretation suggests a description of the electronic structure where the spreading of the energy levels of the manifold leads to the formation of *effective* band-like peaks in the density of states (DOS) (Figure 2b, shaded gray area). The DOS of the 3G4/K⁺ wire thus appears similar to those of materials with a dispersive band structure.

It is important to note that there is a one-to-one correspondence between the band structure and the ground-state conduction properties (e.g., the quantum conductance spectrum) of a periodic system in the coherent transport regime:⁴⁰ at any given energy, the quantum conductance is a constant value proportional to the number of transmitting channels available for charge mobility, which are equal (in the absence of external leads) to the number of bands at the same energy. Therefore, the formation of effective dispersive bands in the investigated G4 wire is a signal of the *intrinsic* capability of the material of hosting electron “energy channels” available for charge migration, within continuous energy ranges. On the contrary, the energy spikes that would characterize a discrete spectrum would not be efficient for transport. The extended orbitals (see below) related to the effective bands turn out to be the corresponding viable “space channels” for carrier mobility, e.g., the pathways through which the carriers may migrate in the wire.

A comparison between the manifolds of the isolated G quartet and of the G4 wire highlights an increased density of energy levels in the manifolds of the quadruple helix with respect to the tetrad. This effect is due to two factors: (i) the number of energy levels in each multiplet; (ii) the in-plane and out-of-plane guanine–guanine and guanine–metal interactions, which couple the electron states stemming from the various structural elements (either from G or from K) in the supercell. The number of electron states in each manifold depends on the number of molecules and ions in the unit cell: therefore, whereas each manifold of the G quartet contains four levels, the manifolds of the 3G4/K⁺ wire contain twelve levels from the twelve guanines, and additional twelve levels from the K⁺ ions in the energy range where metal–base hybridization occurs. We come back to this point later when we discuss the DOS. The number of levels in a manifold is not the only element that determines the details of the bandstructure: another key feature is the bandwidth, which is instead controlled by the specific interactions. Whereas in the case of the G4 tetrad only H-bonding plays a role, in the case of the 3G4/K⁺ wire there are different contributions from H-bonding and stacking between the bases, and from the coupling between the bases and the metal ions. It is worth noting that the formation of dense manifolds and the consequent establishment of *effective band-like* potential conduction channels is a common characteristic of stacked H-bonded nucleobase aggregates. In fact, not only did we identify the same features in guanine quadruplexes in both the presence and absence of inner metal cations,²⁷ but also similar energy manifolds were detected in the electronic band structure of two different DNA duplexes.^{7,8a,37} For instance, in their simulation of an eleven base-pair poly(dG)–poly(dC)^{8a} sequence, de Pablo and co-workers found a HOMO manifold derived from the eleven states of guanines. In that case, the topmost valence band had a bandwidth of only 40 meV, smaller than that calculated in our G4 wire (~700 meV). This confirms that, though the splitting of the energy levels into multiplets is a fingerprint of stacked rotated H-bonded nucleobases, the peculiar characteristic of the manifolds depends on the intrinsic stacking properties (e.g., the π – π coupling) of each type of helix.

To investigate more closely the effects of the metal cations and of the metal–molecule interaction, we projected⁴¹ the total density of states of 3G4/K⁺ (shaded gray area in Figure 2b) on G (thin red curve) and K (thick blue curve) atomic orbitals. The G- and K-projected DOS's (PDOS's) show that in a large portion of the spectrum (below –2 eV and above 3.5 eV) only the guanine electron states contribute to the DOS. For instance, the LUMO peak at 3.5 eV has a *pure* guanine character, being

the convolution of only the twelve LUMO orbitals of the twelve G's. The contribution of the K⁺ ions to the total DOS is mainly localized at the top of the valence band (between –2 and 0 eV). The presence of both guanine and potassium contributions to the DOS (as seen from the superposition of the blue and red peaks in Figure 2b) at the top of the occupied bands is the consequence of a metal–molecule interaction. The HOMO peak of the 3G4/K⁺ wire (see the double-peak indicated by an arrow in Figure 2b) is due to a convolution of 24 electron states deriving from the coupling between the twelve G HOMO's and the twelve potassium orbitals. Indeed, one would expect that the K⁺ ions would contribute to the DOS only with the filled p orbitals, after the s electrons are removed upon ionization of the system. However, if this were the case, by counting the levels in the manifolds we would find only nine completely occupied levels due to the metal (three p orbitals from each K ion), in addition to the guanine-based manifolds containing twelve levels each. Instead, the number of computed occupied levels (twelve more than those coming from the guanine counting, and all concentrated in the HOMO double-peak) and the occurrence of partial occupation for some of them (those around the computed Fermi level, see Figure 2b) indicates sp hybridization in potassium when inserted in the helical guanine complex. Therefore, potassium does not contribute separately with the 4s and the filled 3p shells, but with a partially occupied sp shell: seven equivalent electrons in four orbitals, which become six electrons in four orbitals when the system is ionized as the 3G4/K⁺ wire. Consequently, the highest energy component of the HOMO double peak has an occupation factor of 3/4, the Fermi level is pinned at the top of the effective valence band (Figure 2b) and the G4 wire in the presence of K⁺ ions behaves as an intrinsically p-type doped system. The observation of delocalized holes at the topmost valence band is in agreement with the description of the electronic structure of potassium discussed above, where each ionized K⁺ atom contributes to the whole electronic structure not with three fully occupied p-levels, but with four partially occupied sp states.

The spread sp orbitals of potassium easily interact with the surrounding molecular orbitals of the tetrads, giving hybrid metal–molecule states. We visualized this effect by drawing the convolution of the effective HOMO of the wire. Figure 3a shows an isosurface of the HOMO charge density in the unit cell, obtained from the convolution of the 24 highest occupied orbitals that contribute to the HOMO double peak. By comparison with Figure 1b, it is possible to recognize a uniform distribution of the π orbitals deriving from the tetrads, but also the inner delocalized density stemming from the orbitals of the K⁺ ions. By cutting the HOMO charge density with a plane perpendicular to the G quartets, we further inspect the features of the metal–molecule interaction (Figure 3b). Due to the high degree of charge delocalization along the wire axis, the G4 wires may be described as good electron/hole channels for mobile charges. Two types of pathways for such mobile charges can be identified in Figure 3b and contribute to the conductivity channels. The first one stems from the low-energy component of the HOMO double peak, is extended through the guanine core of the helix, and is due to the base–base interaction. Similar channels are also observed for the other manifold-derived peaks (e.g., LUMO) and in the empty (K free) quadruple helix.²⁷ The second type of pathway is due to the high-energy component of the HOMO peak and results from the metal–base interaction. This *hybrid* pathway is centered around the potassium ions in the central cavity of the wire, and it clearly shows the coupling

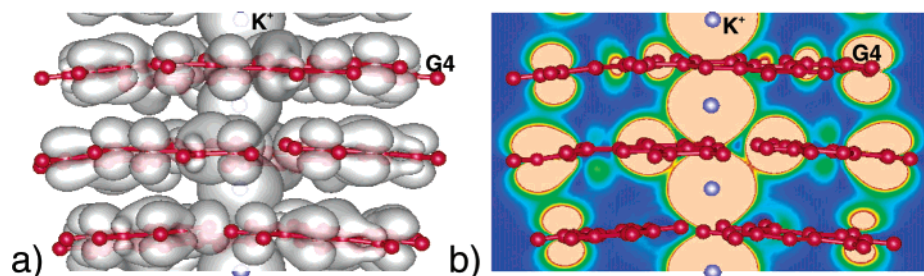


Figure 3. (a) Isosurface plot of the convolution of orbitals that represents the HOMO manifold of the G4 wire, side view. (b) Contour plot of the same orbital in a plane perpendicular to the tetrameric planes and containing the K^+ ions.

with the coordinated oxygen atoms of the G molecules. Hence, the inclusion of the metal cations inside the helix drastically influences the electronic properties of the system. The details of the metal–nucleobase interactions depend on the nature of the cation included in the helix. In the present case of potassium, its coupling with the G bases modifies the topmost valence band, favoring the formation of extended orbitals along the stacking direction and enhancing the conduction properties of the empty guanine structure.²⁷

To gain further insight into the metal–base coupling, we compared the 3G4/ K^+ wire with other two similar neutral systems: the empty quadruple helix (labeled 3G4) and the G4 wire with neutral K atoms (labeled 3G4/K). The structures 3G4 and 3G4/K do not describe real systems but are useful models for better understanding the 3G4/ K^+ quadruplexes. The changes of the inner core do not basically modify the geometry (bond lengths and angles) of the quadruple helix but affect the electronic structure. Figure 4 shows the comparison among the DOS (shaded gray areas) and the PDOS (thin red and thick blue curves) of the systems. To compare the three structures, we aligned the bottom energy levels and fixed the origin of the energy scale at the top of the valence band of the empty 3G4 helix (taken as reference), with the purpose to outline the effects of the inclusion of metals into the empty guanine supramolecular structure.

As already mentioned, in the DOS of all the studied G4 wires we observe the occurrence of broad G-derived peaks, reflecting the same guanine aggregation state. The empty tube has the valence band completely occupied and the Fermi level lays in the middle of the gap; in the presence of potassium (3G4/K and 3G4/ K^+), the Fermi level is pinned at the top of a partially occupied valence band. In the 3G4 case, the HOMO peak is the convolution of the HOMO's of guanines (H_G in Figure 4), which are completely occupied; in the other two cases, instead, the HOMO derives from the interactions between the HOMO's of guanine (H_G) and the hybrid states of potassium (labeled K in Figure 4), which are partially filled. One may consider the 3G4/K structure as obtained by adding three electrons to the 3G4/ K^+ . The inclusion of such electrons increases (from 3/4 to 7/8 filling factor) but does not complete the occupation of the topmost band; thus, the helix with the atomic K would also be an intrinsic p-type doped wire.

By analyzing the position and the width of the band-like peaks for the three systems, we can underline further details about the K–G interactions. As the K-derived states are found at the top of the valence band, far away from that range the spectra are identical; e.g., peaks a, b, e, and f have the same width, shape, and positions in the three plots. Also the G-like LUMO peak L_G remains basically unchanged. On the contrary, in the 3G4/ K^+ wire (central panel in Figure 4) the occurrence of a nonvanishing K–PDOS in the $[-2; -1]$ eV range strongly modifies peaks c and d with respect to the empty wire: the

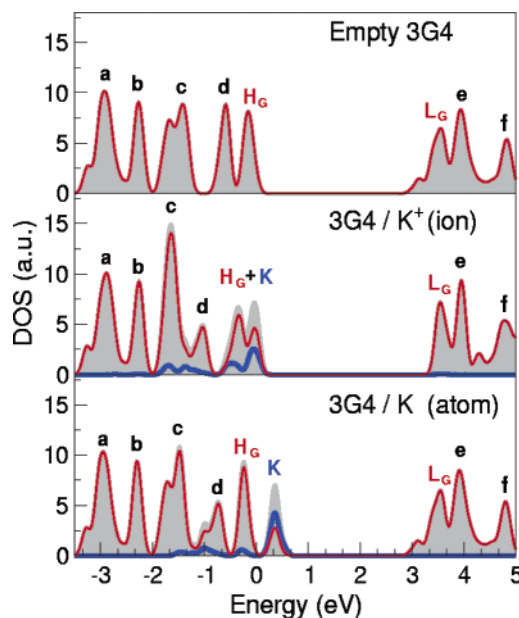


Figure 4. Total and projected density of states (DOS) of different quadruple helical G4 wires: without inner metal (3G4) in the top panel, with K^+ ions (3G4/ K^+) in the middle panel, with neutral K atoms (3G4/K) in the bottom panel. In each panel, the shaded gray area represents the total DOS, the thin red (thick blue) curve marks the contribution of guanine (potassium) to the DOS. H_G (L_G) labels the band-like peak deriving from the HOMO's (LUMO's) of single guanine molecules in the unit cell. The label K identifies peaks with a pronounced potassium contribution. The origin of the energy scale is consistently set at the HOMO of the empty column in the three plots. The 3G4 is an insulator with a large HOMO–LUMO gap. In the metal-containing quadruplexes 3G4/ K^+ and 3G4/K, instead, the Fermi level is pinned at the top of the $H_G + K$ and of the K peaks, respectively, due to partially occupied electron states.

electrostatic coupling between the σ -like peak d and the sp orbitals of the K^+ ions shifts the position of this peak to lower energies and reduces its height. All the other peaks in Figure 4 have a π -like character and are less influenced by the G– K^+ coupling. The displacement of peak d also modifies peak c, which is sharper and higher in 3G4/ K^+ than in the free-standing tube. In the neutral 3G4/K helix, the electrostatic coupling between K and G is more effectively screened because of the larger number of electrons in the system: as a consequence, the shift of peak d is reduced with respect to the 3G4/ K^+ case, and peak c remains similar to that of the empty wire. Another difference that we remark is the composition of the HOMO peaks: whereas for the 3G4 empty tube the HOMO is purely G-like (H_G), it is a mixed G–K-like double-peak ($H_G + K$) for the charged 3G4/ K^+ wire. For the neutral 3G4/K wire, the HOMO (Figure 4, middle panel) is split into two sharper peaks (Figure 4, bottom panel): a lower energy component similar to the peak H_G and a higher component with a prevalent K

character. The decrease in the degree of K–G orbital mixing in 3G4/K with respect to 3G4/K⁺ is most likely attributable to the increased occupation of the sp shell of potassium, which becomes more inert because more similar to a closed shell.

These changes in the electronic structure due to different charge states of the inner metals underline the delicate equilibrium that rules the stability and the mutual interactions in this hybrid organic/inorganic molecule/metal complex. Differently from M-DNA,¹³ where the metal cation substitutes for an imino hydrogen atom and is covalently bonded to a nucleobase, in G4 wires there is no direct charge sharing between the metal and the guanines. The stability and the electronic properties of the system are ruled by the coordination ratio among the K⁺ and the eight nearest-neighboring oxygen atoms, symmetrically located above and below the ion (Figure 1c). The metal cations not only stabilize the structure via electrostatic interactions but also constitute an *effective bridge* between the electronic charge density around the oxygen atoms: the HOMO contour plot shown in Figure 3b is the result of the π – π coupling between the oxygens of consecutive tetrads, mediated by the electronic structure of the K⁺ ion.

The possibility of changing the electronic properties of the G4 wire, by using different metal ions to stabilize the stack, is expected to be a powerful tool for tuning the conduction properties of the nanowires. We are currently exploring the inclusion of other cations with different outer-shell electronic configurations (e.g., the transition metals), which may be exploited to further change the conductivity of G4 wires.

4. Conclusions

The first-principles study of the electronic and conduction properties of infinite G4 wires, stabilized by K⁺ inner cations, shows that the π – π coupling among stacked planar tetrads is insufficient to induce the formation of dispersive bands in the wires. However, the presence of closely spaced energy levels leads to the formation of manifolds, whose density of states suggests a band-like behavior. The coupling among guanine-localized molecular orbitals, which may be easily induced by a weak external interaction, gives rise to extended electron channels, suitable to host mobile charge carriers along the wire.

Although the formation of split manifolds seems to be a general feature of base–base interactions in H-bonded stacked supramolecular nucleobase aggregates, the effects due to the presence of the metals depend on the identity of the cations. In the case of potassium, the inclusion of the cations enhances the conduction properties of the system, generating additional extended electronic channels stemming from the metal–guanine interaction. The mixed sp orbitals of K⁺ hybridize with the HOMO's of guanine, and this coupling gives origin to a partially filled HOMO band, which makes the system equivalent to a p-doped wide-band gap semiconductor.

The above results, along with their attractive mechanical and self-assembly properties, suggest that G4 wires may be explored as viable DNA-based conductors for nanoscale molecular electronics. The computed properties are the equivalent of those of a bulk material: of course, the actual behavior as a wire in a device setting depends on the specific device implementation, is affected from conditions such as electrode–wire and substrate–wire coupling, and leaves several open issues for further investigation and exploitation.

Acknowledgment. We gratefully thank Joshua Jortner for illuminating discussions. This work was supported by the EC through project “DNA-based nanowires” IST-2001-38951, by

INFM through “Progetto calcolo parallelo” which provided computer time at CINECA (Bologna, Italy), and by MIUR (Italy) through grant “FIRB-NOMADE”.

References and Notes

- (1) (a) Joachim, C.; Gimzewski, J. K.; Aviram, A. *Nature* **2000**, *408*, 541–548. (b) Heath, J. R.; Ratner, M. A. *Phys. Today* **2003**, *56*, 43–49.
- (2) Seeman, N. C. *Nature* **2003**, *421*, 427–431.
- (3) Niemeyer, C. M. *Angew. Chem. Int. Ed.* **2001**, *40*, 4128–4158.
- (4) Yan, H.; Zhang, X.; Shen, Z.; Seeman, N. C. *Nature* **2002**, *415*, 62–65.
- (5) (a) Braun, E.; Eichen, Y.; Sivan, U.; Ben-Yoseph, G. *Nature* **1998**, *391*, 775–778. (b) Keren, K.; Krueger, M.; Gilad, R.; Ben-Yoseph, G.; Sivan, U.; Braun, E. *Science* **2002**, *297*, 72–75. (c) Warner, M. G.; Hutchison, J. E. *Nature Mater.* **2003**, *2*, 272–277.
- (6) Dekker, C.; Ratner, M. A. *Phys. World* **2001**, *8*, 29–34.
- (7) Porath, D.; Cuniberti, G.; Di Felice, R. To be published in *Long-range charge transfer in DNA*; Schuster, G., Ed.; Springer-Verlag: Berlin.
- (8) (a) de Pablo, P. J.; Moreno-Herrero, F.; Colchero, J.; Gómez-Herrero, J.; Herrero, P.; Baró, A. M.; Ordejon, P.; Soler, J. M.; Artacho, E. *Phys. Rev. Lett.* **2000**, *85*, 4992–4995. (b) Storm, A. J.; van Noort, J.; de Vries, S.; Dekker, C. *Appl. Phys. Lett.* **2001**, *79*, 3881–3883.
- (9) (a) Porath, D.; Bezryadin, A.; de Vries, S.; Dekker, C. *Nature* **2000**, *403*, 635–638. (b) Cai, L.; Tabata, H.; Kawai, T. *Appl. Phys. Lett.* **2000**, *77*, 3105–3107.
- (10) Fink, H.-W.; Schönenberger, C. *Nature* **1999**, *398*, 407–410.
- (11) Kasumov, A. Yu.; Kociak, M.; Guéron, S.; Reulet, B.; Volkov, V. T.; Klinov, D. V.; Bouchiat, H. *Science* **2001**, *291*, 280–282.
- (12) Richter, J. *Physica E* **2003**, *16*, 157–173.
- (13) Rakitin, A.; Aich, P.; Papadopoulos, C.; Kobzar, Yu.; Vedenev, A. S.; Lee, J. S.; Xu, J. M. *Phys. Rev. Lett.* **2001**, *86*, 3670–3673.
- (14) Tanaka, K.; Tengeiji, A.; Kato, T.; Toyama, N.; Shionoya, M. *Science* **2003**, *299*, 1212–1213.
- (15) The term *G wire* has previously appeared in the literature to label quadruple helices deriving both from guanine rich sequences (e.g., G₄T₂G₄) and from lipophilic guanosine monomers. In this paper we will use *G4 wire* to describe the four-stranded homoguanilyc rods.
- (16) (a) Alberti, P.; Mergny, J. L. *Proc. Natl. Acad. Sci. U.S.A.* **2003**, *100*, 1569–1573. (b) Li, J. J.; Tan, W. *Nano Lett.* **2002**, *2*, 315–318.
- (17) Saenger, W. *Principles of Nucleic Acids*, Springer-Verlag: New York, 1984.
- (18) Gottarelli, G.; Spada, G. P.; Garbesi, A. In *Comprehensive Supramolecular Chemistry*; Atwood, J. L.; Davies, J. E. D., MacNicol, D. D., Vögtle, F., Eds.; Pergamon: Oxford, U.K., 1996; Vol. 9.
- (19) (a) Marlow, A. L.; Mezzina, E.; Spada, G. P.; Masiero, S.; Davis, J. T.; Gottarelli, G. *J. Org. Chem.* **1999**, *64*, 5116–5123. (b) Kotch, F. W.; Fetting, J. C.; Davis, J. T. *Org. Lett.* **2000**, *2*, 3277–3280.
- (20) (a) Williamson, J. R.; Raghuraman, M. K.; Cech, T. R. *Cell* **1989**, *59*, 871–880. (b) Parkinson, G. N.; Lee, M. P. N.; Neidle, S. *Nature* **2002**, *417*, 876–880. (c) Dapić, V.; Abdomerović, V.; Marrington, R.; Peberdy, J.; Rodger, A.; Trent, J. O.; Bates, P. J. *Nucl. Acids Res.* **2003**, *31*, 2097–2107.
- (21) (a) Laughlan, G.; Murchie, A. I. H.; Norman, D. G.; Moore, M. H.; Moody, P. C. E.; Lilley, D. M. J.; Luisi, B. *Science* **1994**, *265*, 520–524. (b) Phillips, K.; Dauter, Z.; Murchie, A. I. H.; Lilley, D. M. J.; Luisi, B. *J. Mol. Biol.* **1997**, *273*, 171–182. X-ray structure ID UDF062.
- (22) (a) Aboul-ela, F.; Murchie, A. I. H.; Norman, D. G.; Lilley, D. M. J. *J. Mol. Biol.* **1994**, *243*, 458–471. (b) Rovnyak, D.; Baldus, M.; Wu, G.; Hud, N. V.; Feigon, J.; Griffin, R. G. *J. Am. Chem. Soc.* **2000**, *122*, 11423–11429.
- (23) (a) Schultze, P.; Hud, N. V.; Smith, F. W.; Feigon, J. *Nucl. Acids Res.* **1999**, *27*, 3018–3028. (b) Marathias, V. M.; Bolton, P. H. *Biochemistry* **1999**, *38*, 4355–4364. (c) Basu, S.; Szewczak, A. A.; Cocco, M.; Strobel, S. A. *J. Am. Chem. Soc.* **2000**, *122*, 3240–3241. (d) Wong, A.; Fetting, J. C.; Forman, S. L.; Davis, J. T.; Wu, G. *J. Am. Chem. Soc.* **2002**, *124*, 742–743. (e) Crnugelj, M.; Hud, N. V.; Plavec, J. *J. Mol. Biol.* **2002**, *320*, 11423–11429.
- (24) (a) Deng, J.; Xiong, Y.; Sundaralingam, M. *Proc. Natl. Acad. Sci. U.S.A.* **2001**, *98*, 13665–13670. (b) Shi, X.; Fetting, J. C.; Davis, J. T. *J. Am. Chem. Soc.* **2001**, *123*, 6738–6739. (c) Miyoshi, D.; Nakao, A.; Sugimoto, N. *Nucl. Acids Res.* **2003**, *31*, 1156–1163.
- (25) (a) Marsh, T. C.; Vesenska, J.; Henderson, E. *Nucl. Acids Res.* **1995**, *23*, 696–700. (b) Porath, D. Private communication.
- (26) (a) Töhl, J.; Eimer, W. *Biophys. Chem.* **1997**, *67*, 177–186. (b) Špačková, N.; Berger, I.; Šponer, J. *J. Am. Chem. Soc.* **1999**, *121*, 5519–5534. (c) Gu, J.; Leszczynski, J. *J. Phys. Chem. A* **2000**, *104*, 6308–6313. (d) Gu, J.; Leszczynski, J. *J. Phys. Chem. A* **2002**, *106*, 529–532. (e) Chowdhury, S.; Bansal, M. J. *J. Phys. Chem. B* **2001**, *105*, 7572–7578. (f) Meyer, M.; Steinke, T.; Brandl, M.; Sühnel, J. *J. Comput. Chem.* **2001**, *22*, 109–124. (g) Louit, G.; Hocquet, A.; Ghomi, M.; Meyer, M.; Sühnel, J. *PhysChemCommun* **2003**, *6*, 1–5.

- (27) Calzolari, A.; Di Felice, R.; Molinari, E.; Garbesi, A. *Appl. Phys. Lett.* **2002**, *80*, 3331–3333.
- (28) Wimmer, E. In *Density Functional Approaches for Molecular and Materials Design*; Laird, B. B., Ross, R. B., Ziegler, T., Eds.; American Chemical Society, Washington, DC, 1996; p 423.
- (29) Perdew, J. P.; Chevary, J. A.; Vosko, S. H.; Jackson, K. A.; Pederson, M. R.; Singh, D. J.; Fiolhais, C. *Phys. Rev. B* **1992**, *46*, 6671–6687.
- (30) Friesner, R. A.; Dunietz, B. D. *Acc. Chem. Res.* **2001**, *34*, 351–358.
- (31) (a) Di Felice, R.; Calzolari, A.; Molinari, E.; Garbesi, *Phys. Rev. B* **2002**, *65*, 045104. (b) Calzolari, A.; Di Felice, R.; Molinari, E.; Garbesi, A. *Physica E* **2002**, *13*, 1236–1240.
- (32) We used the code PWSCF by S. Baroni, A. Dal Corso, S. de Gironcoli, P. Giannozzi, available at <http://www.pwscf.org>.
- (33) Vanderbilt, D. *Phys. Rev. B* **1990**, *41*, 7892–7895.
- (34) Troullier, N.; Martins, J. L. *Phys. Rev. B* **1992**, *46*, 1754–1765.
- (35) Louie, S. G.; Froyen, S.; Cohen, M. L. *Phys. Rev. B* **1982**, *26*, 1738–1742.
- (36) (a) Ladik J. J.; Ye, Y.-J. *Phys. Stat. Solidi (b)* **1998**, *205*, 3–10. (b) Ye, Y.-J.; Jiang, Y. *Int. J. Quantum Chem.* **2000**, *78*, 112–130.
- (37) Gervasio, F. L.; Carloni, P.; Parrinello, M. *Phys. Rev. Lett.* **2002**, *89*, 108102.
- (38) (a) Lee, H.-Y.; Tanaka, H.; Otsuka, Y.; Yoo, K.-H.; Lee, J.-O.; Kawai, T. *Appl. Phys. Lett.* **2002**, *80*, 1670–1672. (b) Das, R.; Mills, T. T.; Kwok, L. W.; Maskel, G. S.; Millett, I. S.; Doniach, S.; Finkelstein, K. D.; Herschlag, D.; Pollack, L. *Phys. Rev. Lett.* **2003**, *90*, 188103.
- (39) (a) Adessi, Ch.; Walch, S.; Anantram, M. P. *Phys. Rev. B* **2003**, *67*, 081405(R). (b) Adessi, Ch.; Anantram, M. P. *Appl. Phys. Lett.* **2003**, *82*, 2353–2355.
- (40) Datta, S. *Electronic transport in mesoscopic systems*; Cambridge University Press: Cambridge, U.K., 1995.
- (41) The G projection was obtained by summing over the projections onto the atomic orbitals of all the species contained in the guanine molecules.